QCD critical point sweep during black hole formation

A. Ohnishi[*], H. Ueda[†], T. Z. Nakano[†,*], M. Ruggieri[*] and K. Sumiyoshi[**]

[*]*Yukawa Institute for Theoretical Physics, Kyoto University, Kyoto 606-8502, Japan*
[†]*Department of Physics, Faculty of Science, Kyoto University, Kyoto 606-8502, Japan*
[**]*Numazu College of Technology, Ooka 3600, Numazu, Shizuoka 410-8501, Japan*

Abstract. We discuss the possibility to probe the QCD critical point during the prompt black hole formation. In black hole formation processes, temperature and baryon chemical potential become as high as $T \sim 90$MeV and $\mu_B \sim 1300$MeV. This high baryon chemical potential would allow nuclear matter to experience the QCD phase transition, and the temperature may be higher than the QCD critical point temperature. We compare the phase boundary in chiral effective models and the thermal environment obtained in the ν radiation hydrodynamical calculation of the gravitational collapse of a $40M_\odot$ star leading to the black hole formation. This comparison suggests that quark matter is likely to be formed, and the QCD critical point may be swept.

Keywords: QCD critical point, black hole formation, chiral effective models
PACS: 25.75.Nq, 97.60.-s, 12.39.Fe

INTRODUCTION

There are two important aspects in nuclear matter physics related to compact stars — the equation of state (EOS) and the phase diagram. Nuclear matter EOS [1, 2, 3] is an important ingredient in describing compact astrophysical objects such as neutron stars, supernovae, black hole formation, and neutron star merger. The nuclear matter phase diagram is another interesting facet [4]. The discovery of the liquid-gas phase transition may be one of the most successful achievements in observing the phase transition in subatomic physics. The non-monotonic behavior in the caloric curve signals the first order nature of the liquid-gas phase transition [5]. Recent high-energy heavy-ion experiments provide evidence that the created matter is opaque for colored partons, very hot in the early stage, and has specific transport properties. This form of matter is referred to as the strongly coupled quark-gluon plasma (sQGP) [6]. It is generally believed that we have at least one more type of phase transition in nuclear matter; phase transition to quark matter at high density, which is expected to be the first order, while the transition observed in high-energy heavy-ion collisions at $\mu_B \simeq 0$ is the cross over.

The QCD critical point (CP) [7] is one of the main physics goals in the beam energy and system size scan programs at RHIC and SPS [8]. CP would be probed in these experiments if it is in the low baryon chemical potential region, $\mu_{\rm CP} \lesssim 500$ MeV, as predicted in some of the lattice MC calculations [9]. On the other hand, we cannot reject the possibility that the CP is located in the lower T and higher μ_B region, as predicted in many of the chiral effective models [10, 11, 12, 13], which is consistent with the lattice MC calculation at imaginary chemical potential suggesting that CP does not exist in the

small μ_B region [14]. Thus, it is valuable to consider other candidate sites where hot and dense matter is formed and CP is reachable.

For the hunting of CP in the large μ_B region, black hole formation from a gravitational collapse of a massive star is promising. A large part of non-rotating massive stars with mass $M \gtrsim 20M_\odot$ are expected to collapse to black holes (BH) without violent explosion [15]. In the neutrino-radiation hydrodynamical simulations of the collapse and bounce stage of a $40M_\odot$ star leading to a BH, hot $(T \sim 90\ \mathrm{MeV})$, dense $(\rho_B \sim 4\rho_0)$, and highly isospin asymmetric $(Y_p \sim 0.2)$ matter is formed. Thermodynamical variables as a function of radius form a curve in the $(T, \mu_B, \delta\mu)$ space (BH formation profile). In the left panel of Fig. 1, double lines show the BH formation profile $(T, \mu_B, \delta\mu)$ [16] calculated by using the Shen EOS at $t = 0.5, 1.0$ and 1.344 sec after the bounce during the BH formation from a 40 $M_\odot$ star in the proto-neutron star core. From the outer to the inner region of the proto-neutron star, T first increases and reaches $T \sim (50 - 90)$ MeV in the middle heated region, and decreases again inside. The baryon chemical potential μ_B is found to go over 1300 MeV in the central region just before the horizon formation at $t = 1.344$ sec. The isospin chemical potential is found to be $\delta\mu \equiv (\mu_n - \mu_p)/2 = (50 - 130)$ MeV in the inner region. The temperature and density in BH formation are significantly higher than those in supernovae. The highest temperature and density are moderate in the collapse and bounce stage of supernovae, $(T, \rho_B) \sim (21.5\ \mathrm{MeV}, 0.24\ \mathrm{fm}^{-3})$ when hadronic EOS is adopted [3], while it has been argued that the transition to quark matter might trigger successful supernovae [17]. Since both T and ρ_B are larger during BH formation compared with the supernova explosions, it is likely to create a new form of matter, such as the dense quark matter.

In this proceedings, we discuss here the possibility that the BH formation profile evolves with time and may pass through CP and the vicinity (*CP sweep*) [18]. The CP location scatters in the $T-\mu_B$ plane in chiral effective models. We expect that CP moves in the lower T direction at finite $\delta\mu$, because d-quark dominates and the effective number of flavors decreases. Since the matter passes through the high μ_B and low T region compared with high-energy heavy-ion collisions, the reduction of the CP temperature T_{CP} is essential for the CP sweep during the BH formation.

CHIRAL EFFECTIVE MODELS

Chiral effective models of QCD have been extensively utilized to study the phase transition at finite μ region; we have the sign problem in lattice QCD MC simulations at finite μ, which makes it difficult to predict the phase boundary at large μ/T, and we need to invoke effective model approaches or some approximation such as the strong coupling expansion [19] in order to investigate the whole phase diagram.

We compare the results of the Nambu-Jona Lasinio (NJL) model [10], the Polyakov loop extended Nambu-Jona-Lasino (P-NJL) model [11], P-NJL model with eight-quark interaction (P-NJL$_8$) [12], and the Polyakov loop extended quark-meson (PQM) model [13]. We here briefly summarize the Polyakov loop extended quark meson (PQM) model, as an example of chiral effective models. The Lagrangian density in PQM is

given by

$$\begin{aligned}\mathscr{L} =&\bar{q}\left[i\gamma^\mu D_\mu - g(\sigma + i\gamma_5 \boldsymbol{\tau}\cdot\boldsymbol{\pi}) - g_v\gamma^\mu(\omega_\mu + \boldsymbol{\tau}\cdot\boldsymbol{R}_\mu)\right] q \\ &+\frac{1}{2}(\partial_\mu\sigma)^2 + \frac{1}{2}(\partial_\mu\boldsymbol{\pi})^2 - U(\sigma,\boldsymbol{\pi}) - \mathscr{U}_\ell(\ell,\bar{\ell},T) \\ &-\frac{1}{4}\omega_{\mu\nu}\omega^{\mu\nu} - \frac{1}{4}\boldsymbol{R}_{\mu\nu}\cdot\boldsymbol{R}^{\mu\nu} + \frac{1}{2}m_v^2(\omega_\mu\omega^\mu + \boldsymbol{R}_\mu\cdot\boldsymbol{R}^\mu)\ . \end{aligned} \tag{1}$$

Compared with the NJL model, PQM has a freedom to choose the mesonic potential, $U(\sigma,\boldsymbol{\pi}) = \lambda\left(\sigma^2+\boldsymbol{\pi}^2-v^2\right)^2/4 - h\sigma$. We have introduced the coupling of quark and vector mesons, whose kinetic part is given by the field tensors, $\omega_{\mu\nu}$ and $\boldsymbol{R}_{\mu\nu}$ for ω and ρ mesons, respectively. The Polyakov loop is the order parameter of the deconfinement transition and is defined as $\ell = \mathrm{Tr}[\mathscr{P}\exp(i\int_0^{1/T} d\tau A_4)]/N_c$, and its effective potential is chosen to be $\mathscr{U}_\ell(\ell,\bar{\ell},T) = T^4[-a(T)\bar{\ell}\ell/2 + b(T)\log H(\ell,\bar{\ell})]$, where H represents the Haar measure.

The thermodynamic potential in the mean field approximation is obtained as

$$\begin{aligned}\Omega_{\mathrm{PQM}} =&U_\sigma + \mathscr{U}_\ell - \frac{g_v^2}{m_v^2}\left(\rho_u^2+\rho_d^2\right) - 2N_fN_c\int^\Lambda \frac{d^3\boldsymbol{p}}{(2\pi)^3}E_p \\ &-2T\sum_f\int\frac{d^3\boldsymbol{p}}{(2\pi)^3}\left[\log\mathscr{R}(E_p-\tilde{\mu},\ell,\bar{\ell}) + \log\mathscr{R}(E_p+\tilde{\mu},\bar{\ell},\ell)\right]\ , \end{aligned} \tag{2}$$

where $E_p = \sqrt{\boldsymbol{p}^2+M^2}$ and $M = g\sigma + m_0$ is the constituent quark mass. The vector meson effects are included in the effective chemical potential $\tilde{\mu}_f = \mu \mp \delta\mu - 2g_v^2\rho_f/m_v^2$ with $\mp = -,+$ for $f = u$ and d, respectively. We here adopt the three-momentum cutoff Λ in evaluating the zero point energy for simplicity. Model parameters are fixed to reproduce hadron properties in vacuum and lattice MC results on the temperature dependence of the Polyakov loop, while the vector coupling is taken as a free parameter [18].

ASYMMETRIC MATTER PHASE DIAGRAM AND CRITICAL POINT SWEEP DURING BLACK HOLE FORMATION

By solving the stationary conditions with respect to the chiral condensate σ and the Polyakov loop $(\ell,\bar{\ell})$, we obtain the equilibrium state for given $(T,\mu_B,\delta\mu)$. At zero μ_B, the equilibrium values of σ and the Polyakov loop evolve smoothly as increasing T, showing the cross over transition. At zero T, we find the first order phase transition at the transition baryon chemical potential $\mu_B = N_c\mu = \mu_c$, where σ jumps from a large value around f_π to a small value. In the left panel of Fig. 1, we show the first order phase boundary in the 3D space $(T,\mu_B,\delta\mu)$ in PQM. The first order phase boundary is found to shrink at finite $\delta\mu$. Transition temperature at a given baryon chemical potential μ_B decreases, and the transition baryon chemical potential μ_c at $T=0$ also decreases. This behavior is understood as a consequence of effective flavor number reduction; the phase transition is weaker for smaller number of flavors, and d quark is favored but u quark is disfavored at finite $\delta\mu > 0$.

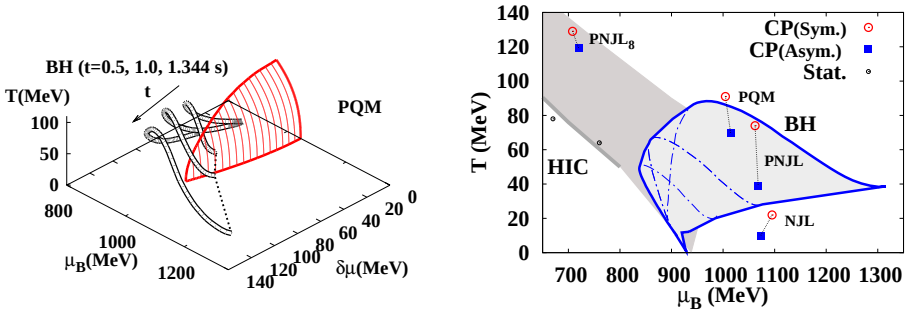

FIGURE 1. Left: First order phase boundary surface (solid lines) in $(T, \mu_B, \delta\mu)$ space calculated with the PQM model are compared with the BH formation profile, (thermodynamical variables $(T, \mu_B, \delta\mu)$ during the BH formation) at $t = 0.5, 1.0, 1.344$ sec after the bounce (double lines) [18]. Right: Predictions of the critical temperature and critical point locations in symmetric and asymmetric ($\delta\mu = 50$ MeV) matter in comparison with the chemical freeze-out points in heavy-ion collisions [20] and the (T, μ_B) region swept during the black hole formation.

In the right panel of Fig. 1, we show the CP location in symmetric ($\delta\mu = 0$) and asymmetric ($\delta\mu = 50$ MeV) matter obtained in NJL [10], P-NJL [11], P-NJL with 8-quark interaction (P-NJL$_8$) [12], and PQM [13] models. As already mentioned, the CP location is sensitive to $\delta\mu$. Compared with the results in symmetric matter, $T_{\rm CP}$ is smaller at finite $\delta\mu$ and reaches zero at $\delta\mu = \delta\mu_c \simeq (50 - 80)$ MeV. CP is also sensitive to the form of the Lagrangian and model parameters. Single quark excitations are suppressed in the hadron phase by the Polyakov loop, then we obtain higher transition temperature and the critical temperature in P-NJL compared with the NJL model. The vector potential shifts the chemical potential effectively, and shifts up the transition chemical potential μ_c by about 10-15 MeV at $g_v/g = 0.2$. Because of these sensitivities, effective models would be strongly constrained once the CP location is specified by any means.

We shall now compare the CP location and the phase boundary with the BH formation profile. In the left panel of Fig. 1, we compare the phase boundaries and the BH formation profile in PQM. During the BH formation, the baryon chemical potential reaches around 1000, 1100 and 1300 MeV in the central region of the proto-neutron star at $t = 0.5, 1.0$ and 1.344 sec, respectively [16, 18]. The transition chemical potential is calculated to be $\mu_c = (1000 - 1100)$ MeV in the models discussed here, then it is likely that quark matter is formed between $t = 0.5$ and 1.0 sec in the central region.

We find that there are three types in the quark matter formation — the first order transition, the crossover transition, and the CP sweep, where the BH formation profile goes below, above and through the critical line in asymmetric matter. In the case of the first order transition, we have three (hadronic, co-existing, and quark matter) layers in the proto-neutron star, while there is no layer structure when the quark matter is formed via cross over transition. The second bang scenario is based on the first order transition. In the cross over formation, the pressure suppression is not expected, and the horizon formation may be delayed. In the CP sweep case, the three layers merges to be one at the time of CP sweep. Depending on the EOS in the mixed phase, we may have some kind of instability of the layer structure.

Finally we discuss the phase transition in neutron stars. The reduction of $T_{\rm CP}$ in

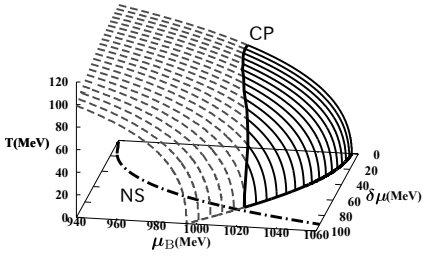

FIGURE 2. Phase boundary surface in $(T, \mu_B, \delta\mu)$ space in PQM (solid lines for the first order transition, and dashed lines for cross over transition) and the neutron star matter chemical potential $(\mu_B, \delta\mu)$ in Shen EOS (dot-dashed line).

asymmetric matter results in the disappearance of the first order transition at large $\delta\mu$ even at $T = 0$. If this applies to neutron star matter, the pressure reduction is weakened at the phase transition. This may be related to the existence of 2 solar mass neutron star [21]. In Fig. 2, we compare the phase boundary surface in PQM with the $(\mu_B, \delta\mu)$ relation in neutron star matter obtained in Shen EOS [2]. We find that the isospin chemical potential in neutron stars is large enough, where the first order phase transition disappears when we take the vector-scalar coupling ratio $g_v/g = 0.2$. It should be noted that, however, this result is sensitive to the model details and probably to the existence of inhomogeneous phases [22].

SUMMARY AND DISCUSSION

In this proceedings, we have discussed the possibility to probe the high baryon chemical potential (μ_B) region of the QCD phase diagram during the prompt black hole (BH) formation. We have compared the phase boundary obtained in the chiral effective models with the thermodynamical variables $(T, \mu_B, \delta\mu)$ in the neutrino-radiation hydrodynamical calculation of gravitational collapse of a 40 $M_\odot$ star leading to black hole formation. For this comparison, we find that the nuclear matter asymmetry or the isospin chemical potential $\delta\mu$ plays an important role. The present work is based on the comparison of the hydrodynamical simulation results using hadronic EOS with the phase boundary in chiral effective models of quarks. While it is desired to compare the results using the combined EOS which is applicable both in hadronic phase and quark-gluon phase, the present comparison is relevant provided that the combined EOS respects the known properties of nuclear matter EOS at low T and μ_B.

The transition chemical potential in symmetric matter at $T = 0$ is found to be in the range of $\mu_c = (1000 - 1110)$ MeV in the chiral effective models considered here. We can compare these values with the highest baryon chemical potential realized during the BH formation, $\mu_B = 1300$ MeV. Thus it is probable that quark matter is formed during the BH formation. We have found that there are three types in transition to quark matter during the BH formation. When the thermodynamical trajectory go below, above, or through CP in asymmetric matter, the QCD phase transition proceeds via the first order transition, the cross over transition, or the CP sweep. Observational consequence of the CP sweep is not clear. In the talk, we argued that three layers of quark, mixed,

and hadronic matter in the proto-neutron star merges to one layer at a time when CP is swept. In order to obtain quantitative results, it is necessary to examine the results using the combined EOS. Once the CP location is specified, it constraints the model Lagrangian form and parameters strongly.

ACKNOWLEDGMENTS

This work was supported in part by Grant-in-Aid for Scientific Research from JSPS and MEXT (Nos. 22-3314, 22540296), the Grant-in-Aid for Scientific Research on Innovative Areas from MEXT (No. 20105004), the Yukawa International Program for Quark-hadron Sciences (YIPQS), and by Grants-in-Aid for the global COE program 'The Next Generation of Physics, Spun from Universality and Emergence' from MEXT.

REFERENCES

1. J. M. Lattimer and F. D. Swesty, Nucl. Phys. A **535** (1991) 331.
2. H. Shen, H. Toki, K. Oyamatsu and K. Sumiyoshi, Nucl. Phys. A **637** (1998), 435; Prog. Theor. Phys. **100** (1998), 1013.
3. C. Ishizuka, A. Ohnishi, K. Tsubakihara, K. Sumiyoshi and S. Yamada, J. Phys. G **35** (2008), 085201.
4. See for example, A. Ohnishi, Prog. Theor. Phys. Suppl., to appear [arXiv:1112.3210 [nucl-th]].
5. J. Pochodzalla *et al.*, Phys. Rev. Lett. **75**, 1040 (1995).
6. M. Gyulassy and L. McLerran, Nucl. Phys. A **750**, 30 (2005).
7. M. Asakawa and K. Yazaki, Nucl. Phys. A **504** (1989) 668; M. A. Stephanov, Prog. Theor. Phys. Suppl. **153**, 139 (2004).
8. See for example, G. Odyniec, Acta Phys. Polon. B **40** (2009) 1237; N. Abgrall *et al.* [NA61 Collaboration], PoS CPOD **2009** (2009) 049.
9. Z. Fodor, S. D. Katz, JHEP **0404** (2004) 050; S. Ejiri *et al.*, Prog. Theor. Phys. Suppl. **153** (2004) 118; A. Li, A. Alexandru and K. -F. Liu, Phys. Rev. D **84** (2011) 071503.
10. Y. Nambu and G. Jona-Lasinio, Phys. Rev. **122** (1961) 345; *ibid* **124** (1961) 246; T. Hatsuda and T. Kunihiro, Phys. Rept. **247** (1994) 221.
11. K. Fukushima, Phys. Rev. D **68** (2003) 045004; S. Roessner, C. Ratti and W. Weise, Phys. Rev. D **75** (2007) 034007.
12. K. Kashiwa, H. Kouno, M. Matsuzaki and M. Yahiro, Phys. Lett. B **662** (2008) 26.
13. V. Skokov, B. Friman, E. Nakano, K. Redlich and B. J. Schaefer, Phys. Rev. D **82** (2010) 034029.
14. P. de Forcrand and O. Philipsen, JHEP **0701** (2007) 077; JHEP **0811** (2008) 012. C. Bonati, P. de Forcrand, M. D'Elia, O. Philipsen and F. Sanfilippo, arXiv:1201.2769 [hep-lat].
15. S. J. Smartt, J. J. Eldridge, R. M. Crockett and J. R. Maund, MNRAS **395** (2009) 1409 [arXiv:0809.0403 [astro-ph]]; K. 'i. Nomoto, N. Tominaga, H. Umeda, C. Kobayashi and K. Maeda, Nucl. Phys. A **777** (2006) 424.
16. K. Sumiyoshi, S. Yamada, H. Suzuki and S. Chiba, Phys. Rev. Lett. **97** (2006) 091101; K. Sumiyoshi, C. Ishizuka, A. Ohnishi, S. Yamada and H. Suzuki, Astrophys. J. Lett. 690 (2009) 43; K. 'i. Nakazato *et al.*, Astrophys. J., in press [arXiv:1111.2900 [astro-ph.HE]].
17. T. Hatsuda, Mod. Phys. Lett. **A2** (1987) 805; I. Sagert *et al.*, Phys. Rev. Lett. **102** (2009) 081101.
18. A. Ohnishi, H. Ueda, T. Z. Nakano, M. Ruggieri and K. Sumiyoshi, Phys. Lett. B **704** (2011) 284.
19. T. Z. Nakano, K. Miura and A. Ohnishi, Prog. Theor. Phys. **123** (2010) 825; Phys. Rev. D **83** (2011) 016014; K. Miura, T. Z. Nakano, A. Ohnishi and N. Kawamoto, Phys. Rev. D **80** (2009) 074034; K. Miura, T. Z. Nakano and A. Ohnishi, Prog. Theor. Phys. **122** (2009) 1045.
20. A. Andronic, P. Braun-Munzinger and J. Stachel, Nucl. Phys. A **772** (2006) 167.
21. P. Demorest, T. Pennucci, S. Ransom, M. Roberts and J. Hessels, Nature **467** (2010) 1081.
22. E. Nakano and T. Tatsumi, Phys. Rev. D **71** (2005) 114006; D. Nickel, Phys. Rev. D **80** (2009) 074025; T. Kojo, Y. Hidaka, L. McLerran and R. D. Pisarski, Nucl. Phys. A **843** (2010) 37.